

**Directional Reflectance Characterization Facility
and Measurement Methodology**

B.T. McGuckin, D.A. Haner, R.T. Menzies, C. Esproles and A.M. Brothers

**Jet Propulsion Laboratory
California Institute of Technology
4800 Oak Grove Drive
Pasadena CA 91109**

Abstract

A precision reflectance characterization facility, constructed specifically for the measurement of the hi-directional reflectance properties of Spectralon panels planned for use as in-flight calibrators on the NASA Multi-angle Imaging SpectroRadiometer (MISR) instrument is described. The incident linearly polarized radiation is provided at three laser wavelengths: 442 nm, 632.8 nm and 859.9 nm. Each beam is collimated when incident on the Spectralon. The illuminated area of the panel is viewed using a silicon photodetector which revolves around the panel (360°) on a 30 cm boom extending from a common rotational axis. The reflected radiance detector signal is ratioed with that from a reference detector to minimize the effect of amplitude instabilities in the laser sources. This and other measures adopted to reduce noise have resulted in a BRDF calibration facility with a precision regarding the measurement of hi-directional reflection function (BRF) measurement precision of 0.002 at the 10 confidence level. The Spectralon test piece panel is held in a computer controlled three axis rotational assembly capable of full 360° rotation in the horizontal plane and 90° in the vertical. The angular positioning system has repeatability and resolution of 0.0010. Design details along with an outline of the measurement methodology are presented.

1. Introduction

The Multi-angle Imaging SpectroRadiometer (MISR) is presently being designed and constructed at the Jet Propulsion Laboratory (JPL) as an Earth observing System (EOS) flight instrument scheduled for launch in 1998. MISR will obtain global multi angle radiometrically calibrated imagery from a suite of nine cameras pointed toward the Earth, each at a unique angle, and at four spectral bands per camera. In order to meet the requirement that an absolute radiometric calibration be maintained to within 3% uncertainty throughout the five year mission life, a key part of the instrument is an On-Board Calibration (OBC) sub-system⁽¹⁾. Integral to the OBC are a pair of deployable, diffuse panels which will be deployed at approximately monthly intervals over the poles to reflect solar irradiance into the cameras for in-flight calibration. The diffuse reflectance panels will be made from Spectralon, a Labsphere Inc. proprietary organic compound capable of satisfying the demands of nearly Lambertian reflectance, spatial uniformity and predictable bidirectional reflection function (BRF)⁽²⁾. Several Spectralon panels have been the subject of comprehensive series of pre-flight tests of the material optical reflectance characteristics⁽³⁾ as part of a comprehensive MISR Calibration exercise undertaken at JPL.

It is the purpose of this paper to report on the detailed design and operation of a facility constructed specially for the measurement of the bi-directional reflectance properties of Spectralon panels with the objectives of quantifying spatial uniformity, reflectance isotropy and integrated hemispheric reflectance and depolarization characteristics. The design features and diagnostics utilized to achieve and verify system performance are highlighted.

2. Facility Description

The facility is similar in many respects to other such systems^(4,5,6) which either use conventional light sources and filter combinations or lasers for the illumination of materials of interest. The optical layout is diagrammed in Figure 1. The characterization of the Spectralon panels takes place at three wavelengths, each of which is chosen to be close to one of the four MISR spectral bands. Designated bands L1, L2 and L3, the prescribed requirement is that L1 be within $\pm 5\text{nm}$

of 443 nm, L2 is within 555 - 670 nm, and L3 must be within ± 10 nm of 865 nm. In this facility, the three wavelengths chosen are all derived from laser sources: a helium cadmium (HeCd) laser at a wavelength of 442 nm, a helium neon (HeNe) laser at 632.8 nm and a gallium aluminum arsenide (GaAlAs) semiconductor diode laser source at 859.9 nm. The output from each laser of chosen size and polarization is passed through an optical train and onto the panel surface. All optical surfaces of the elements in the path are dielectrically coated for operation at each specific wavelength in order to minimize scatter, depolarization (all coatings are for p-polarized light relative to the table surface) and for optimum throughput. Where possible, the optical mounts are fixed in place; however, self-positioning mounts are used wherever the optical path would be blocked for another wavelength. These mounts have proven to have excellent reproducibility in repositioning.

The requirement for precision of ± 0.001 at the 1σ confidence level in each of the BRF measurements (0.1% of the reflected signal for each angle pair) demands low noise optical irradiance and detector / amplifier electronics. The former is addressed by the use of low noise, stable sources and also the deployment of a spatial filter (SF) / Keplerian telescope combination in the beam path for the elimination of higher order spatial frequencies and to improve the signal to noise ratio. At 859.9 nm following collimation and circularization of the diode laser output using high numerical aperture lenses and an anamorphic prism pair, the beam diameter is too large to pass efficiently through the microscope objective lens of the spatial filter; therefore another objective lens is used.

3. Incident Beam Preparation

The calibration test plan calls for an effective illuminated area of one inch in diameter actual physical size on the Spectralon surface and a maximum angle of incidence $\theta_i = 60^\circ$. Rather than change the beam size for each of the three specified angles of incidence (30° , 45° and 60°), the incident beam diameter is selected such that the physical size condition is satisfied at $\theta_i = 60^\circ$ with the penalty of reduced illuminated area when $\theta_i = 30^\circ$ and 45° . Therefore, the diameter of the collimated beam incident on the Spectralon target is 1.27 cm (0.5 inches).

The image lens of the Keplerian telescope is unique to each wavelength and chosen to provide the required half-inch diameter beam at the output taking into account each incident laser beam diameter (HeCd = 1 mm, HcNe = 0.48 mm and GaAlAs = 8 mm), divergence and laser-to-SF distance. Afocal alignment is readily achieved by manual translation of the image lens on a precision rail.

The beam telescope component parameters are listed in Table 1. In all cases, the anti-reflection coated lenses are off-the-shelf components selected for a convenient lens separation and clear aperture (38.1 mm) to accommodate the 12.7 mm diameter collimated beam. The lenses are plano convex, mounted with the convex surfaces toward the collimated beam to minimize aberrations. In Table 1, D_{in} is the incident beam diameter, f_{in} and f_{out} are respectively the telescope input and output lens focal lengths, f_{out}/f_{in} is the required telescope magnification for an emergent collimated beam of diameter D_{out} . The optimum pinhole diameters are 5 and 25 μm respectively at 442 nm and 632.8 nm.

4. Detector Optical Telescope Design

The MISR Spectralon Optical Test Plan requires that the detector should resolve the radiant exitance to less than 2° , and that an effective illuminated area be one inch in diameter at the maximum angle of incidence. Both requirements influence the optical design of the telescope placed in front of the viewing detector which was designed and fabricated specifically for this task and is shown in Figure 2.

The detector resolution, Θ , is determined by the ratio, of r , the aperture stop (1 cm) to s , the radial distance of the stop from the Spectralon panel (30 cm) and is given by:

$$\Theta = \left(\frac{r}{s}\right) = 1.9'' \text{ (Full}\angle\text{)}$$

Mechanical stability is an important factor which had to be considered in the choice of detector

boom length: the greater the length the more difficult it is to minimize flexing of the boom and the associated movement of the image on the detector surface, with concomitant added noise and uncertainties. This was avoided by selecting a boom length of 30 cm and fabricating the boom from a length of aluminum channel for added stiffness.

The 1" major axis of the area of the panel to be imaged and the detector FOV are defined by the field stop diameter (0.56 cm) and the distance of the field stop from the lens (6.29 cm). See Figure 3. While it is important that the detector over samples the illuminated area on the panel, the imaged area should be as close as practicable to the actual illuminated area in order to minimize the amount of stray light incident imaged onto the detector.

Solving the similar triangles for I, the diameter of the panel area imaged by the telescope gives:

$$\left(\frac{I}{30}\right) = \left(\frac{FS}{6.29}\right) \Rightarrow I = 2.67 \text{ cm}$$

The telescope images onto the detector an area on the SpectraIon panel which is 2.67 cm (1.05 inches) in diameter. As required, this is greater than the size of the illuminated area even when the panel is oriented at 60° angle of incidence (where the ellipse major axis is 2.54 cm) and also at 30° and 45° angles of incidence when the illuminated area is comfortably over sampled. Care was taken to avoid the possibility of vignetting of the beam at the detector by modeling the size of the imaged field at the detector at extreme view angles. At a view angle of 70°, the imaged field parameters are calculated for beam incidence angles of 30, 45 and 60° and there is no vignetting of the imaged beam by the 1 cm square detector under any conditions although there is a change of image shape and a slight loss of focus at the extreme view angle (700).

A narrow (10 nm) bandpass "line" filter with peak transmission at each wavelength channel is positioned in front of each of the signal and reference detector telescopes. This minimizes the background noise effects of ambient lighting, resulting in attenuation of greater than 40 dB. The reference signal detector assembly is further enclosed in a black anodized shroud to avoid the

possibility of sensing light scattered from the panel or from other surfaces.

5. Target and Detector Motion Control.

Accurate knowledge of the Spectralon panel and detector locations is required, with the objective of acquisition at 10 sampling, with $\pm 0.5^\circ$ accuracy in repeatability of view position. Further, there is the additional requirement that the view range must be able to view from 0° to $+75^\circ$ in both the principal plane, defined by the detector axis and the incident beam, and at any azimuthal angle.

This level of performance is achieved by using commercially available rotary stages which control the detector and target rotation. Both are capable of 360° rotation with 0.0010 resolution. Bi-directional repeatability is 0.003° , accuracy 0.05° and backlash is below 0.05° . A goniometric cradle is used to position the target elevation angle (in the laboratory frame of reference). This is capable of $\pm 45^\circ$ travel and 0.010 resolution. Two mounting adapters have been designed and built which allow the target to be positioned in such a way as to allow $+ \text{ or } -90^\circ$ tilt in and out of the principal plane.

All stages have high torque dc motors and precision incremental encoders permitting control of target and detector position when interfaced through a control box to a 386 computer. The high torque allows the mechanism to position the heavy panels and associated fixtures rapidly and repeatedly without overshoot.

6. System optical Alignment

Angular resolution capability of 0.5° necessitates careful alignment of the target normal (and therefore the detector position) in the set-up phase of the experiment. This alignment is done optically using an alignment mirror which is positioned securely in the target assembly. The mirror substrate angular wedge (flatness tolerance) is significantly less than 0.5° so that it does not contribute a measurement bias. Measurements of the substrate thickness revealed a parallel

tolerance of 0.002" over the mirror diameter of 1" (corresponding to a wedge angle of ≤ 2 mrad or $\leq 0.11^\circ$).

The alignment of the incident beam onto the SpectraIon panel surface proceeds as follows: At each wavelength and with the panel removed, the incident beam is aligned through two irises along the optical bench at height of 20 cm above the table, both of which straddle the target assembly, see Figure 1. After replacing the target, the mirror adaptor assembly is held in place against the frame of the tray within which the panel is held. Iterative adjustment of the target position is made using control software until the reflected beam (and therefore target normal) retraces the incident beam path through the iris upstream along the incident beam. The reflected beam is measured to be consistently within 0.05° of exact alignment going through this iris.

With the incident beam reflected back upon itself, the target normal is then defined in the control software as being at 0° in both rotation and tilt in the laboratory coordinate system. Control software is then used to check that the target mount rotation assembly is capable of maintaining" the target normal in the principal plane (i.e. that containing the normal and the incident beam). This is done by cycling the target rotation through $\pm 45^\circ$ and $\pm 60^\circ$. At each extreme angle, the reflected beam height is measured and recorded with the radial distance from the target center (axis of rotation). Any tilt above or below the principal plane is then calculated, These results are shown in Table 2. The maximum tilt out of principal plane is $\pm 0.06^\circ$ over target rotation of $\pm 60^\circ$.

The detector reference position is similarly calibrated by using the motion control software to move the detector into position such that the incident beam strikes a reference mark on the rear of the detector housing, thereafter defined as 0° position. The definition of the laboratory frame of reference is dictated by the configuration of the hardware and is unique to the system. The motion control software contains the transformation equations between the laboratory and the standard spherical coordinate system. The menu prompts the system operator for inputs in a laboratory reference frame, but the data are calculated and presented in standard spherical coordinates.

Having established the mechanical integrity of the target positioning hardware, a similar exercise was followed to ensure that the detector is always in the principal plane during its rotation. In this case, the change in height of a reference point on the detector boom is recorded using a height gauge as the detector was rotated over $\pm 90^\circ$. The detector run-out is 0.012 cm over total distance of 76 cm when stowed in the $\pm 90^\circ$ position. This corresponds to the detector being in the principal plane to a tolerance of 0.010 through a detector boom rotation of 180° .

The pointing accuracy of the detector / telescope assembly is also checked to ensure that the detector is always pointed towards the illuminated area of the panel as it is rotated around the panel during typical acquisition scenario. This is done using a specially designed fixture which simulates the detector assembly from which extends a coaxial stylus pointing towards the turning axis of the target which intersects the incident beam path. (This point itself is identified to an accuracy of ± 0.025 cm). The position of the stylus point relative to the turning center is monitored as the detector and target are cycled through a typical measurement run. The stylus point remains on the panel detector turning axis throughout the range of detector and target” movement.

7. Optical Signal Detection and Processing

In order to achieve a maximum precision in the measurement of the BRF the effects of laser output power instability were minimized by the use of two detection channels: a signal channel which views a portion of the light scattered from the Spectralon panel and a reference channel which monitors the laser power incident onto the calibration panel. The reference channel is “polarization decoupled” from the signal beam using a half-waveplate polarizer combination for each wavelength. The extinction ratio of the polarizer is $>500:1$, which ensures the requisite polarization purity of the beam incident on the target. The reference detector assembly is similar to that on the detector boom. The respective signals are recorded and ratioed automatically by the data acquisition software,

All optical signals are measured using 10 x 10 mm square silicon photodiodes with a noise

equivalent power (NEP) of $1.8 \times 10^{-14} \text{ W} \cdot \text{Hz}^{1/2}$. The sensitivity of each detector over all three wavelength bands avoids unnecessary disturbance to the experiment when transitioning between laser sources.

The signal chain is illustrated in Figure 4, which shows that path from each photodiode to the computer data acquisition system is via pre-amplifier (a transimpedance amplifier) and a 5-100kHz lock-in (phase sensitive detection) amplifier. The internal reference oscillators in each are synchronized to further reduce noise and the possibility of any long term drift. The lock-in output (30 msec time constant) is then amplified by a X5 voltage gain low noise, low frequency amplifier. This is then input to a 12-bit, two channel A/D board on a 20 MHz 386 computer. The X5 amplifier prior to digitizing is used to amplify the input signal to the A/D board to operate the digitizer as close as possible to 5V for full-scale operation in order to minimize the contribution of digitizing error on the SNR. The calculated noise voltages contributed by each of the component elements for a typical lock-in sensitivity setting and the resultant rms noise equivalent voltage to the input of the A/D board input are shown in Table 3.

The lock-in amplifier post-detection time constant and the duration of the sampling period specified by the operator, are carefully selected to ensure that calculated and displayed standard deviation for each detection channel (and ratio) give a true representation of the system noise and provide adequate filtering. The post detection time constant and sampling intervals were chosen to be $\tau_c = 30 \text{ ms}$ and 10 ms respectively. Under these conditions, the lock-in is able to provide sufficient "smoothing" of the detector signal with the A/D board sampling three times per τ_c . The lock-in sensitivity is adjusted to produce a voltage signal approximately $\frac{3}{4}$ of full scale of the digitizer for the peak reflectivity panel signals (taking care to avoid saturation) in order to minimize digitizing error.

A special purpose menu-driven software package on a 386 computer is used to record the digitized data for each channel which is summed over an operator defined number of points (usually 1000) for each view angle. The data are processed in real time, and compiled into a unique data file at the end of each run. This file contains the average signal on each of the

detector channels, the calculated standard deviation for each and the signal-to- reference ratio over the user-defined incident and range of view angle. In addition, the target and detector angular locations are also recorded. This can then be printed or displayed, an example of which is shown in Table 4.

The two-axis target and the reflected signal detector motion, together with the digitization rate, and the number of samples per detector position are controlled with a C language program on the personal computer.

8. System operation

Before carrying out any data runs, the operational reproducibility of the setup is periodically checked on a run-to-run basis. This is ascertained by recording several data sets from one panel position several times over a period of one hour during which no adjustments were made to any part of the system. Calculation of the ratio difference between the data files reveals that repeatability is <0.296 . This scope of this test was extended to include further checks following” total electrical shut-down, disassembly of the target and the elapse of several days between runs, In this instance repeatability was measured to be $< 0.4\%$.

The measurement of the Spectralon panel BRF at a wavelength of 632.8 nm as part of the process of quantifying the isotropic panel BRF will serve to illustrate the operation of the system described thus far. The panel initially examined is an “Engineering Model” (EM) version of that which will fly with the MISR instrument. The panel measures 22.5 x 2.5 x 0.25 inches and is contained within an aluminum tray with its location defined by three positioning cleats in the rear of the panel. The tray is mounted into the computer controlled target assembly described above.

Characterization of the panel as isotropic can be made by assuming an optic axis in the material and measuring (he BRF for the two cases where the angle of incidence is fixed but the angle to the optic axis has been changed by 180. Thus the incident beam is in the principal plane but incident from opposing directions with respect to the optic axis. The detector angle was varied

from $-70^\circ \leq \theta_r \leq 70^\circ$ where $\theta_r = 0^\circ$ corresponds to the detector angle at the panel normal. Other similarity symmetric schemes for comparison were obtained by tilting the panel normal by $\pm 30^\circ$ relative to the principal plane and one run was also taken in the principal plane. The angular range for each data run is specified by the user who is prompted for begin, end and incremental steps by the control program. The operator has control over the data sampling: typically at each incremental position of the rotating detector, 1000 samples are recorded in both channels and the sampling interval is set at 10 ms. The data at each view angle are automatically averaged and the mean value and the standard deviation are output in the data file.

The data obtained from these runs is illustrated in Figure 5. The curves are the difference normalized to the average expressed as percent for the two incident directions. It is clear that the three curves *lack correlation* within the $\pm 0.1\%$ criterion. Subsequent analysis reveals that the mis-match between data sets approaches 8% ⁽⁷⁾ and there is generally no viewing angle from which the panel is measured in which the difference between data obtained at the two incidence angles satisfies the isotropy criteria (correlation between data sets within $\pm 0.1\%$). This anisotropy is thought to be a consequence of orbital sanding of the panel surface, part of the final preparation phase. This is considered to leave a helicoid pattern on tile Spectralon surface which deleteriously affects panel reflectance spatial uniformity especially at larger view angles where the surface contribution dominates. This is discussed in more detail elsewhere ⁽⁷⁾.

This measured BRDF anisotropy from the EM Spectralon panels necessitated the introduction of a fourth axis of rotation into the geometry. The system is now capable of target rotation about the surface normal and thereby maintaining the projection of the incident beam onto the panel constant during panel rotation (i.e. $\phi_i = \text{constant}$). The physical size of the flight panels precludes their direct measurement since the degree of rotation possible would be limited by panel interfering with the rotating boom and the table surface. Instead, this will be done using Spectralon test pieces - 7.5 x 5.0 x 0.6 cm in size and cut from the same piece as those proto flight panels. Experiments have established the correlation between the optical response of the test piece and the proto flight panels to be - 0.4% in reflectance function over a large range of experimental conditions. Thus from measurements on the test pieces, which have a direct

relationship to the flight panels further properties of the flight panels can be deduced.

This added degree of freedom facilitates the measurement of absolute hemispherical reflectance of SpectraIon with ϕ_i kept constant. These system changes and measurements will be discussed under a different title (*).

9. Laser Speckle Limitations on SNR

As stated earlier, the optical test plan includes the requirement that the measurement precision of the BRF be 0.001 at the 10 confidence level. However, in any laser-based geometry, laser speckle will act as a limiter to the SNR possible. Speckle is an optical interference effect and is a consequence of the coherent nature of laser light used in this experiment. Surface irregularities on the SpectraIon panel greater than a wavelength in size can be modeled as an ensemble of point sources when illuminated by the laser light, These point sources scatter the radiation with a random set of phase shifts. A locus of constructive and destructive interference points observed by a detector viewing the scattered radiation field gives rise to a spatially non uniform area of illumination. The scale of the spatial uniformity in the far-field is given by the Fraunhofer diffraction formula for the angular width of independent speckle lobes comprising the radiation pattern^(9,10,11). Any movement of the detector (such as to a different azimuthal position) by an comparable to or larger than the speckle lobe dimension causes a different set of speckle lobes to be imaged and, therefore, a variation in signal intensity detected (convolved with the approximate $\cos \theta_r$ variation in panel reflectance). This has the effect of limiting the SNR in the BRF measurement.

The imitation of speckle on SNR is calculated by considering the number of speckle lobes imaged by the detection optics. At a wavelength, λ , of 859.9 nm (worst case), and an illuminated spot on the panel of diameter, $D = 12.7$ mm, the speckle angular lobe diameter is given by:

$$\Phi_s = 2 \lambda / D = 1.4 \times 10^{-4} \text{ (rad)}$$

The detector - panel separation, L , is set at 30 cm by the requirement that the detector resolution $< 2^\circ$. The physical diameter, d_s , of the speckle lobe at the detector telescope which is at a distance L from the panel is therefore given by:

$$d_s = L \Phi_s = 4.2 \times 10^{-5} \quad (\text{m})$$

To achieve an efficient imaging of the speckle pattern onto the detector, a relay lens with a clear aperture of 1 cm is chosen. Since the lens diameter is much larger than the speckle lobe diameter, the lens “aperture averages” over a large number of adjacent lobes. The speckle limited SNR is proportional to the square root of the number of lobes in the aperture (assuming a stationary speckle field) and is shown in Table 3 as a function of angle of incidence and reflection.

The calculated SNR limitation due to speckle is not manifest in the value of the normalized standard deviation calculated and presented for each averaged data set at each view angle (e.g. Table 4). This standard deviation is calculated from a set of consecutive measurements each subject to time-varying speckle fluctuations and other experimental fluctuations on the temporal scale of the averaging time. The value of the observed SNR based on the calculated normalized standard deviation at each angular position, including all sources of noise, is typically 1000:1 at view angles corresponding to maximum panel reflectivity (i.e., maximum detected). The repeatability of a measurement at a given angle on successive scans was described in Section 9 (The repeatability figure is more indicative of the measurement precision as influenced by speckle, as calculated in Table 3.) The angular resolution between data points is 5° which is greater than the detector resolution 2° . Therefore in consequence of the move - stare - move nature of the measurement, the detector views a completely independent set of speckle lobes at each view angle. The small observed values of normalized standard deviation (e.g. Table 4) indicate a very stable system, with a stable speckle pattern for each angular geometry. While the expected fluctuations in signal level due to changes in incident speckle pattern with angle would be observed between adjacent view angles, it is masked to a large degree by a greater change in signal due to the change in panel reflectivity with angle.

The influence of speckle fluctuations could be reduced by introducing further signal averaging corresponding to small variations in the relative angular position of the detector and/or angular orientation of the target while maintaining 5° resolution over the spherical coordinate surface.

10. Conclusions.

A computer controlled facility constructed specially for the measurement of Spectralon BRF in support of the MISR program at JPL has been described. The system is capable of presenting one of three laser wavelengths; 442 nm, 632.8 nm and 859.9 nm with linear polarization (500:1) and beam diameter up to one inch onto a calibration panel measuring 30 x 4 inches. The panel is mounted in a computer controlled three axis rotational assembly capable of full 360° rotation in the horizontal plane and 90° in the vertical with repeatability and resolution of 0.0010. The illuminated area of the panel is viewed using a silicon photodetector which orbits the panel (360°) on a 30 cm long boom extending from a center rotational axis. The reflected radiance detector signal is ratioed with that from a reference detector to mitigate the effect of amplitude instabilities in the laser sources. *The facility precision regarding the measurement of BRF is 0.002 at the 1σ confidence level.*

Acknowledgments:

This work was carried out at the Jet Propulsion Laboratory, California Institute of Technology, under contract with the National Aeronautics and Space Administration (NASA). D.A. Haner is a member of the Chemistry Department, California State Polytechnic University, Pomona CA. The authors would like to acknowledge the technical support of S. Dermenjian and also discussions with C.J.Bruegge and V. Duval

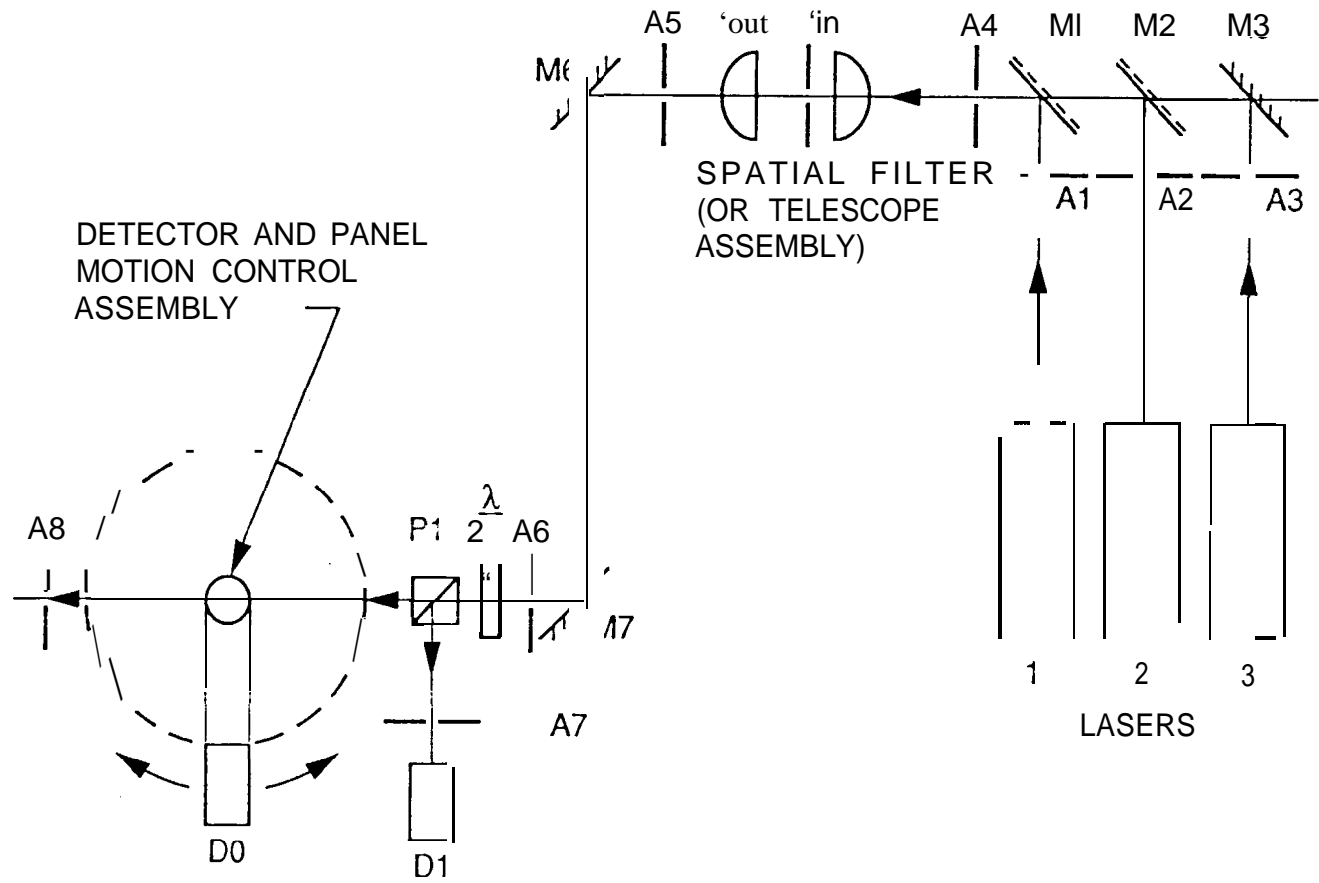
References

1. C.J.Bruegge, A. E. Stiegman, R.A. Rainen and A.W. Springstein "Use of Spectralon as a Diffuse Reflectance Standard for In-Flight Calibration of Earth Orbiting Sensors," Opt. Eng. 32, 805-814 (1993)
2. V.R. Weidner, J.J. Hsia, and B. Adams "Laboratory intercomparison Study of Pressed Polytetra Fluoroethylene Powder Reflectance Standard," Appl. Opt. 24, 2225-2230 (1985)
3. C.J.Bruegge, V. Duval, N.L. Chrien and D.J. Diner "Calibration Plans for the Multi-angle Imaging SpectroRadiometer (MISR)," Metrologia, 30, 213-221 (1993)
4. F.O. Bartell, E. L. Dereniak and W. L.. Wolfe "The Theory and Measurement of Bi-directional Distribution Function (BRDF) and Bi-directional Transmittance Distribution Function (BTDF)," in SPIE 257, 154-160, Radiation Scattering in Optical Systems (1980)
5. B.L. Drolen, "Bi-directional Reflectance and Sulfate Specularity Results for a Variety of Spacecraft Thermal Control Materials" AIAA Thermophysics Conference, 26th, Honolulu, HI, June 1991, Paper 91-1326
6. X. Feng, J.R. Schott and T. Gallagher, "Comparison of Methods for Generation of

Absolute Reflectance-Factor Values for Bi-directional Reflectance Distribution Function Studies,” Appl. Opt., 32, 1234-1242 (1993)

7. 13.'1'. McGuckin and D.A. Haner, “Multi-angle Imaging SpectroRadiometer (MISR): Optical Characterization of the On-Board Spectral on Calibration Panels,” submitted for publication.
8. D.A. Haner, B.T. McGuckin R.T. Menzies, C.J. Bruegge and V. Duval, “The Measurement of The Directional Hemispherical Reflectance from Spectralon,” submitted for publication.
9. M. Françon, *Laser Speckle and Applications in Optics*, Academic Press, New York (1 979)
10. J.C. Dainty (Ed.) “Laser Speckle and Related Phenomena,” in *Topics in Applied Physics*, Vol.8, Springer Verlag, Berlin (1984)
11. J.C. Dainty, “The Statistics of Speckle Patterns,” in *Progress in Optics*, Vol. 14, pp. 1-44, ed. E. Wolf.

Figure 1. Optical layout used for the characterization of the reflectance properties of the Spectralon calibration panels.



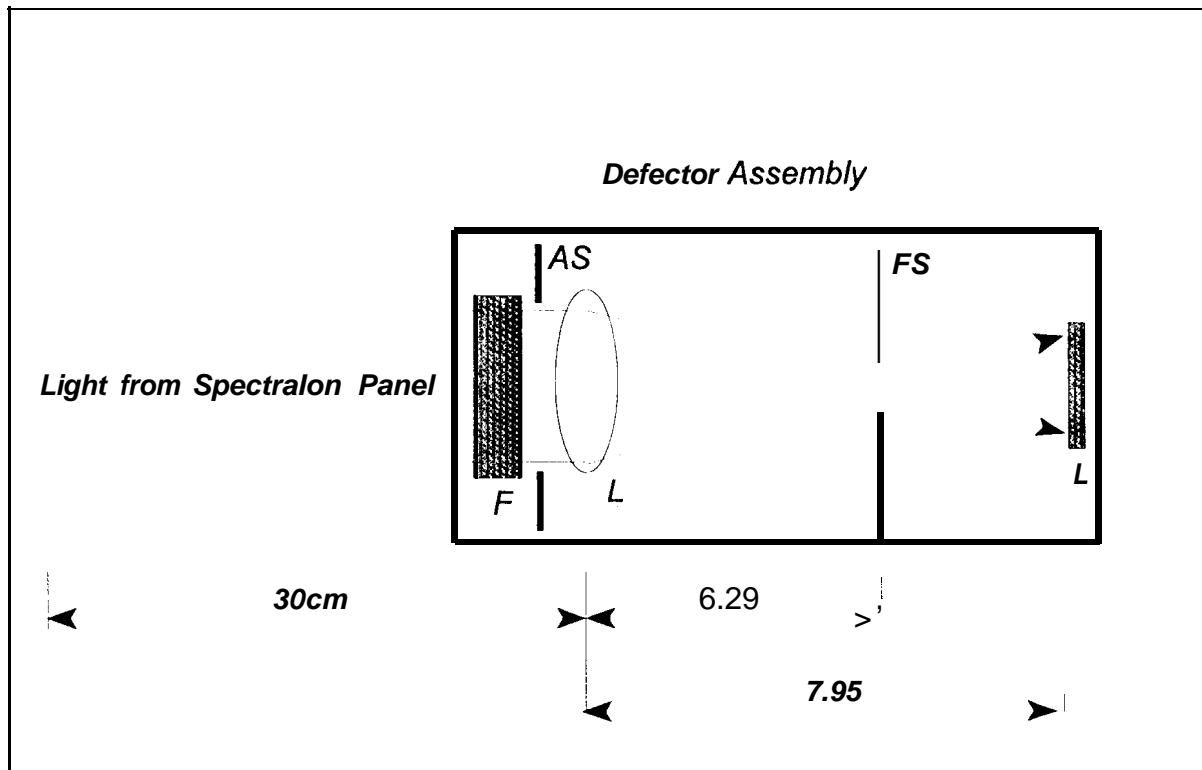


Figure 2. Detector assembly used to view the Spectralon panel and satisfy the imaging requirements. F is one of three notch filters centered at each of the wavelengths, AS is a 1 cm diameter aperture stop, L is the relay lens, FS is a 0.56 cm diameter field stop and D denotes a 1 cm square silicon photodiode. All internal surfaces within the assembly are painted black to minimize scattering.

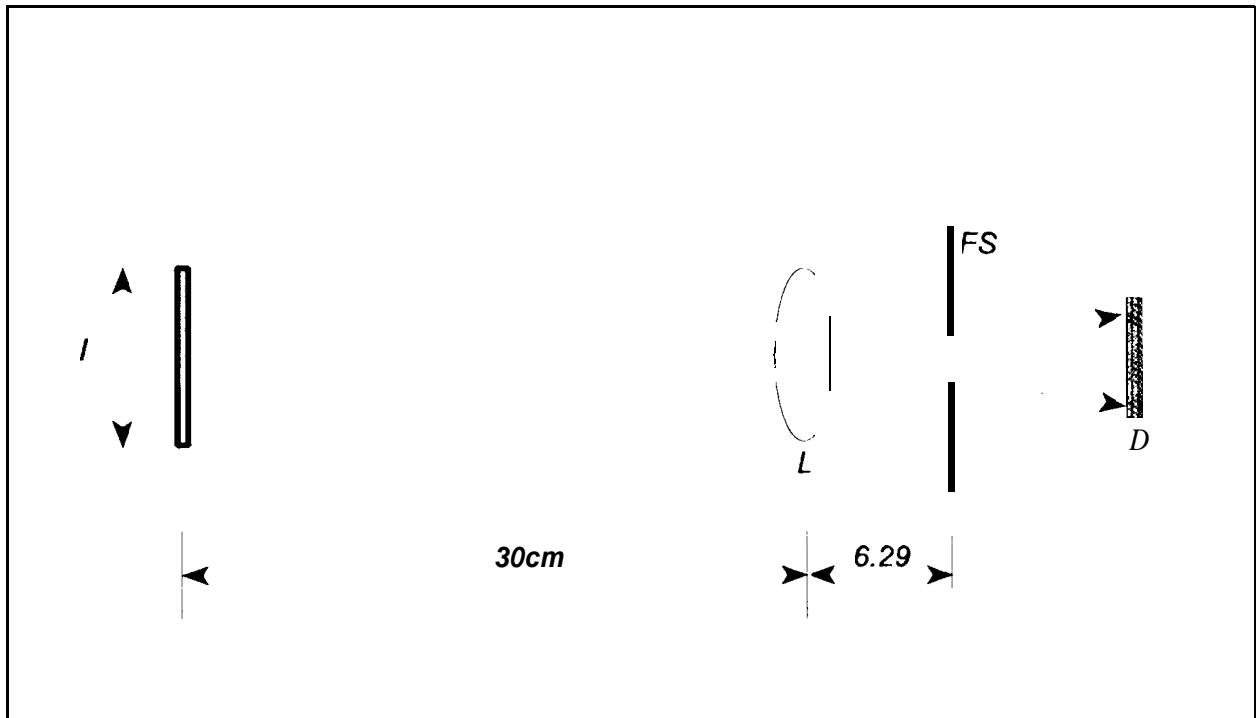


Figure 3. The relative positions of the “I” the area of the panel being imaged by the telescope onto the detector D, the relay lens, L, and the field stop, FS.

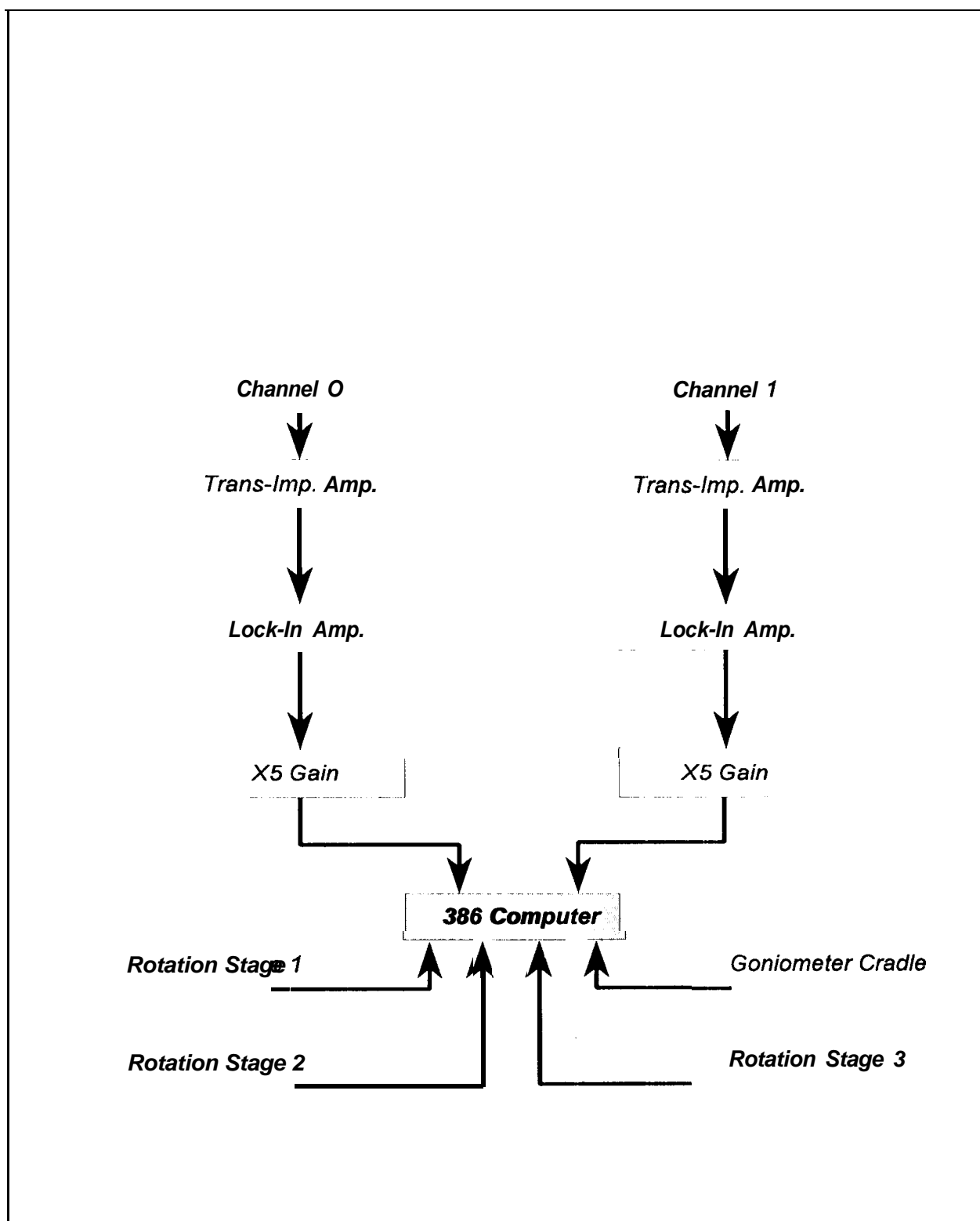


Figure 4. The signal chain for the two detector channels and the interfacing of the motion control hardware with the 386 computer.

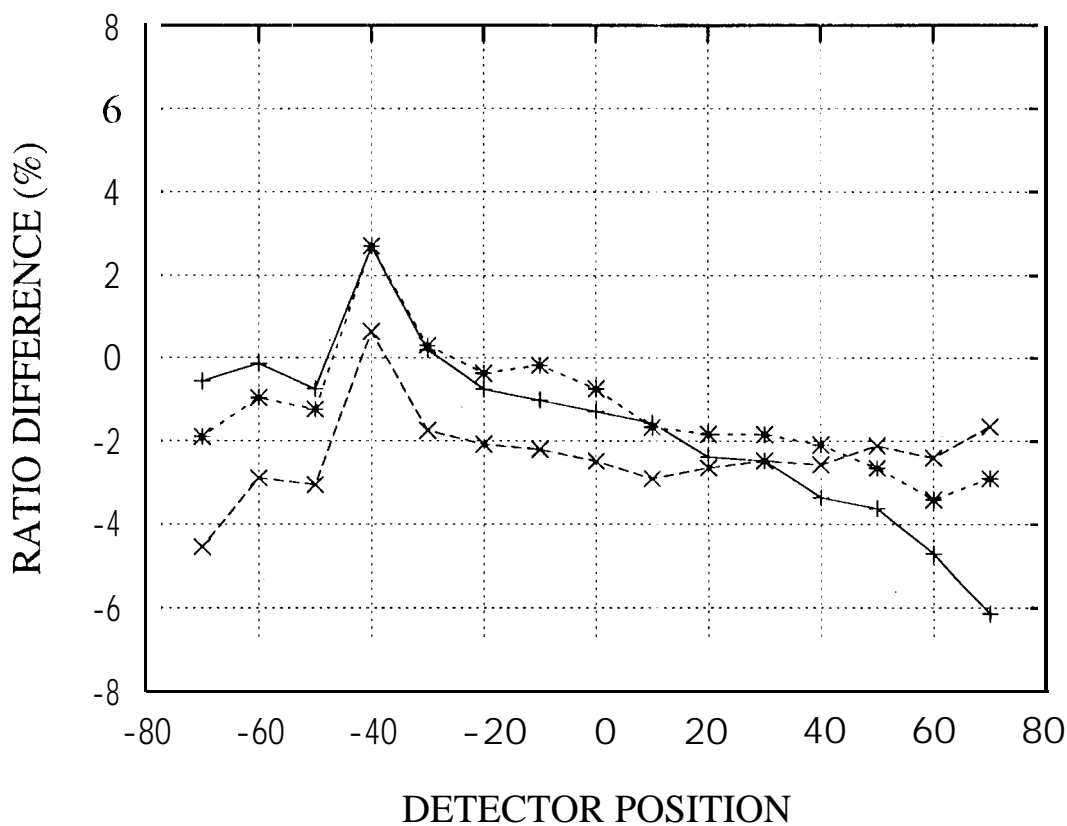


Figure 5. The operational capability of the test setup described in the text is revealed in this plot showing the intercomparison between data files recorded for 859.9 nm with the panel oriented at $\theta_i = 45^\circ$: $\phi_i = 0^\circ$ and 180° . The traces correspond to the cases where the normal to the panel surface is oriented at $+30^\circ$, 0° and -30° relative to the principal plane, Clearly the $\pm 0.1\%$ criterion for panel isotropy is not satisfied. The resultant anisotropy is a consequence of the SpectraIon surface preparation.

k (rim)	D_{in} (mm)	f_{in} (mm)	font (mm)	f_{out}/f_{in}	D_{out} (mm)
442	2.2	14,8	85.4	5.77	12.69
632.8.	3.88	14.8	48.4	3.27	12.69
859.9	8	62.9	100.0	1.59	12.71

Table 1.
Optical system parameters to obtain requisite beam diameter on panel

Incident Angle	Beam Height (in)	Radial Dist. (in)	above/below (\pm)
+45	7.979	22	-0.060°
-45	8,014	20	+ 0.030°
+60	7.985	22	- 0.039°
60	8.020	22	+ 0.042°

Table 2.
Movement of alignment reference above and below the principal plane

Dectector (V)	Amplifier (V)	Lock-in (V)	Amplifier 2 (V)	A / D Board	Total (V)
1.58×10^{-5}	2.52×10^{-4}	2.19×10^{-4}	2.35×10^{-5}	1 bit	3.5×10^{-4}

Table 3.

Calculated noise voltages for the components in the signal chain referred to the A/D Board input.

The A/D has 12 bit resolution with 5 V full scale


```

# name of this file is 94h01 101.741
# JPL CALIBRATION FACILITY          Mon Aug 01 10:17:41 1994
#
# Operator: B: ISO Test; pos'n 6 ;p-pol; tgt "orig" ; det orig;
# Material: Spectralon
# Wavelength: 859.9nm
#
# target elevation          =      -30.000
# target azimuth           =       45.000
# sampling interval (ins) =       10.000
# number of samples/position =      1000
#
#
#
# det      than O      std      than 1      std      mean      std
# position out (v)    dev (V)   out (v)   dev (V)   ratio    dev
70.000    1.44100    0.00160    2.72892    0.00360    0.52805    0.00077
60.000    2.01741    0.00217    2.72986    0.00351    0.73901    0.00106
50.000    2.49151    0.00249    2.72866    0.00390    0.91309    0.00140
40.000    2.89778    0.00285    2.72828    0.00336    1.06213    0.00147
30.000    3.21487    0.00318    2.72923    0.00281    1.17794    0.00145
20.000    3.43302    0.00338    2.72913    0.00281    1.25792    0.00159
10.000    3.56256    0.00346    2.72916    0.00288    1.30537    0.00163
0.000     3.58324    0.00350    2.72826    0.00280    1.31338    0.00164
-10.000   3.52295    0.00357    2.72831    0.00287    1.29126    0.00163
-20.000   3.34325    0.00336    2.72874    0.00293    1.22520    0.00152
-30.000   3.05900    0.00304    2.72849    0.00285    1.12114    0.00140
-40.000   2.73913    0.00277    2.72821    0.00281    1.00401    0.00124
-50.000   2.24011    0.00235    2.72846    0.00282    0.82101    0.00104
-60.000   1.65760    0.00174    2.72803    0.00282    0.60762    0.00075
-70.000   1.07248    0.00163    2.72778    0.00284    0.39317    0.00064

```

Table 4.

Archive data set

	442 nm		632 nm		859 nm	
θ_i	$\theta_r = 0^\circ$	$\theta_r = 70^\circ$	$\theta_r = 0^\circ$	$\theta_r = 70^\circ$	$\theta_r = 0^\circ$	$\theta_r = 70^\circ$
30°	523	179	365	125	269	92
45°	641	219	448	153	329	113
60°	909	310	633	216	465	159

Table S.

Variation in speckle-limited SNR as a function of wavelength, θ_i and θ_r .